Verification of Nonlinear Characteristics of Radar Angular Glint by Surrogate Data Method

Jin Zhang, Zhiping Li, Cheng Zheng, and Jungang Miao

School of Electronic and Information Engineering
Beijing University of Aeronautics and Astronautics, Beijing, 100191, P. R. China
zhangjin850224@139.com, zhiping_li@buaa.edu.cn, zhengcheng@sina.com, jmiaobremen@buaa.edu.cn

Abstract ― In this paper, we present a nontrivial verification of nonlinear characteristics of angular glint by the surrogate data method. Glint is a key cause of target loss in radar detections. Prediction and suppression of glint is a hot topic. Firstly, glint data of a typical target are calculated by GRECO method for two motions. As glint is calculated by quadric surface calculations, it is nonlinear in mathematical nature. The surrogate data method is explained and workflow is summarized to verify the nonlinear traits of glint. Surrogate methods of phase randomized Fourier transform and amplitude adjusted Fourier transform are illustrated. Test statistics of higher order moments and time reversibility are given. Lorenz model is simulated as a standard nonlinear model to verify effectiveness of workflow, and nonlinear verification criteria are drawn. A new parameter is designed to measure the powerfulness of nonlinearity. Finally, nonlinear verifications for the two angular glint series are given. Results are illustrated in figures and data and they agree with nonlinear criterion. This paper lays the foundations for chaotic verifications of glint.

Index Terms ― **A**ngular glint, GRECO, nonlinear verification criterion, and surrogate data method.

I. INTRODUCTION

Since 1959, when the angular glint concept was firstly proposed, it has attracted great interest among electromagnetic diffraction and stealth researchers [1-3]. The primary cause of angular glint is the interaction among each reflection unit of the extended target. When the radar is in operation, angular glint could cause the antenna to jitter, which increases the tracking loss probability. When the target approaches nearer, this phenomenon becomes more evident. Researchers have drawn two conclusions on the relationship between RCS and angular glint: (1) the two are negatively correlative and (2) they are neither correlative nor independent [4-6].

Then two problems arise for further research on glint. The first is how to calculate angular glint precisely; the second is how to verify the nonlinear physical nature of glint and find solutions to suppress glint effects, as several suppression methods such as polarization and frequency diversities have been proposed.

In this paper, for the first problem, we have developed a software package based on phase gradient method (PGM) and GRECO, and glint results are calculated for straight line and rotary motions, which are typical routes across the radar detection range. These results agree well with measurements [7-8]. For the second problem, each angular glint is treated as time series by nonlinear science theories and their nonlinearities are verified by the surrogate data method.

As glint is calculated by nonlinear expressions (quadric surface equations) by GRECO [9], the problem of whether it is nonlinear in physical nature is proposed. The nonlinearity verification is performed in two steps. Firstly, this paper has elaborated the procedures of a known method for diagnosing nonlinearity, the surrogate data method and summarized its workflow, including the surrogate data generations (phase randomized Fourier transform and amplitude adjusted Fourier transform, PRFT and AAFT) and test statistics selection (higher order moments and time reversibility, TC3 and Trev) and their algorithms.

Submitted On: Oct. 31, 2012
Accepted On: Sept. 16, 2013

After that, the results of Lorenz model (publicly accepted nonlinear model) are obtained as a verification of this workflow, and a set of nonlinear verification criterion are proposed. A new parameter (relative length of confidential interval, (RLCI)) to test the powerfulness of nonlinearity is proposed. Secondly, angular glint is verified by the same workflow to verify their nonlinearity. It is apparent that, considering the criterion, angular glint series possess clear nonlinear traits, which is a milestone that points out further chaotic traits of glint.

II. GLINT CALCULATION BY PHASE GRADIENT METHOD AND GRECO

A. GRECO algorithm explanation

As glint is not easily captured in radar detections, theoretical calculation and simulation methods are usually applied. In electromagnetic diffraction theories, any target with more than two scattering centers can generate angular glint. Two types of physical concept are accepted by the majority: the tilt of energy flow [8] and PGM [2], both of which are theoretical. The first is realized by the calculation of the scattering electromagnetic field energy flow; the second is more useful for actual phase measurements of angular glint. It has been verified that in isotropic media and under geometrical optics approximations, the two techniques are identical in physical nature [8].

The GRECO method was developed for RCS real time calculation, and results of several typical targets are given [9]. A similar software has been developed by us, and glint is calculated by PGM [10]. Compared with publicized results, glint calculation accuracies by GRECO are acceptable [10, 11].

In GRECO, each pixel is regarded as a scattering center and all the pixels of a target are calculated, and the angular glint is computed for the target in a trajectory [10]. The calculation setup and target is shown in Fig. 1. In the optical range, the scattering field of the target can be modeled as the vectorial sum of the echo fields of each scattering center. Let d_N be the distance between each scattering center, R and r_N are distances between the center and the radar ($R \approx r_N$), and $R >> d_N$, $R >> \lambda$, the total scattering field received can be derived as,

$$E^S = \sum_{i=0}^{N} E_n^S \exp\left[-j\left(2kr_N - \delta_N\right)\right] \tag{1}$$

where E_n^S and δ_N are the amplitude and phase of the scattering field. The relation between the incident and the scattering field is,

$$\begin{bmatrix} \mathbf{E}_1^s \\ \mathbf{E}_2^s \end{bmatrix} = \begin{bmatrix} \mathrm{Q}_{11} & \mathrm{Q}_{12} \\ \mathrm{Q}_{21} & \mathrm{Q}_{22} \end{bmatrix} \begin{bmatrix} \mathbf{E}_1^i \\ \mathbf{E}_2^i \end{bmatrix} \tag{2}$$

where 1 or 2 denotes vertical or horizontal polarization of the incident or scattering field, and [Q] is the equivalent scattering matrix given by,

$$[\mathbf{Q}] = \mathrm{e}^{\mathrm{i}\varphi_{11}} \begin{bmatrix} \sqrt{\sigma_{11}} & \sqrt{\sigma_{12}}\,\mathrm{e}^{\mathrm{i}(\varphi_{12}-\varphi_{11})} \\ \sqrt{\sigma_{21}}\,\mathrm{e}^{\mathrm{i}(\varphi_{21}-\varphi_{11})} & \sqrt{\sigma_{22}}\,\mathrm{e}^{\mathrm{i}(\varphi_{22}-\varphi_{11})} \end{bmatrix} \tag{3}$$

where $\sigma_{1,2}$ and $\varphi_{1,2}$ are the amplitude and phase of the scattering field for different polarizations. From equation (2), when the incident wave is spherical, the wave front of the scattering field is astigmatic, whose curvature is shown in [Q]. The curvature radii of the scattering fields for two polarizations are given by,

$$\frac{1}{\rho_{1,2}} = \frac{1}{2}\left[\mathrm{Q}_{11} + \mathrm{Q}_{22} \pm \sqrt{\left(\mathrm{Q}_{11} - \mathrm{Q}_{22}\right)^2 + 4\mathrm{Q}_{22}{}^2}\right]. \tag{4}$$

With the target DXF model (perfect conductor) and GRECO, the back-scattering fields are calculated using,

$$\begin{cases} \mathbf{E}_{\perp}^{\mathbf{S}} = \sum_{n=1}^{N} \left(\mathbf{e}_{\mathbf{n}\perp}^{\mathbf{i}} \bullet \mathbf{E}_{\mathbf{n}}^{\mathbf{S}} + \mathbf{e}_{\mathbf{n}\perp}^{\mathbf{i}} \bullet \mathbf{E}_{\mathbf{n}}^{\mathbf{d}}\right) \\ \mathbf{E}_{\parallel}^{\mathbf{S}} = \sum_{n=1}^{N} \left(\mathbf{e}_{\mathbf{n}\parallel}^{\mathbf{i}} \bullet \mathbf{E}_{\mathbf{n}}^{\mathbf{S}} + \mathbf{e}_{\mathbf{n}\parallel}^{\mathbf{i}} \bullet \mathbf{E}_{\mathbf{n}}^{\mathbf{d}}\right) \end{cases} \tag{5}$$

where the scattering field of the n[th] surface and the n[th] edge are represented by $\mathbf{E}_{\mathbf{n}}^{\mathbf{S}}$ and $\mathbf{E}_{\mathbf{n}}^{\mathbf{d}}$, and the total scattering field is their vectorial sum,

$$\mathbf{E}^{\mathbf{S}} = \sum_{n=1}^{N} \left(\mathbf{e}_{\mathbf{n}}^{\mathbf{i}} \bullet \mathbf{E}_{\mathbf{n}}^{\mathbf{S}} + \mathbf{e}_{\mathbf{n}}^{\mathbf{i}} \bullet \mathbf{E}_{\mathbf{n}}^{\mathbf{d}}\right). \tag{6}$$

Under the irradiation of uniformed plane or spherical wave, the beam front of the target is astigmatic, with the phase front of,

$$\phi = \frac{2\pi}{\lambda}\left\{\mathrm{R} + \frac{1}{2}[\mathrm{b}]^{\mathrm{T}}\,\mathrm{Q}(\mathbf{r})[\mathrm{b}]\right\}. \tag{7}$$

In which $[\mathrm{b}]^{\mathrm{T}} = [\mathrm{R}\theta + \mathrm{R}\varphi], [\mathrm{r}, \theta, \varphi]$ is the unit vector in spherical coordinate, Q(R) is the curvature matrix of the scattering wave. The edge and surface scattering centers are all included in GRECO simulations in this paper. The final expressions of angular glint of a complicated target can be given by using the PGM as [11],

$$\begin{cases} e_\theta = \dfrac{r(\nabla\phi)_\theta}{(\nabla\phi)_R} \\ e_\varphi = \dfrac{r(\nabla\phi)_\varphi}{(\nabla\phi)_R} \end{cases} . \quad (8)$$

From equations (7) and (8), angular glint is related not only to R, but also to the astigmatic beam front [b]. These relations are quadric surface expressions, which are typical nonlinear and different from linear differential relations. Therefore, a hypothesis that glint is nonlinear in physical nature when treated as a time series is proposed, and it is verified to be true by the surrogate data method. More importantly, nonlinear is the prerequisite for chaos by nonlinear science theories. These discussions are shown in sections 2 and 3.

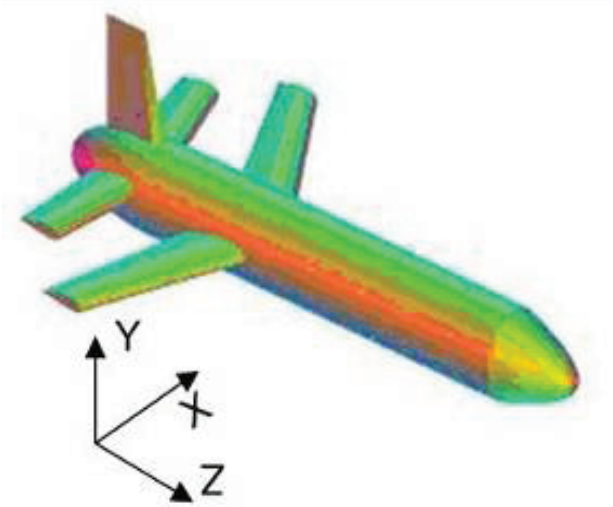

Fig. 1. Target for GRECO simulation [10].

B. Glint calculation by GRECO

The target selected is the same as in [9], and the glint of straight line motion (glint 1) is firstly simulated, which is regarded as the most common trajectory for a target. The motion diagram and results are shown in Figs. 2 and 3.

The second simulation setup is the rotary motion (glint 2), which yields much larger fluctuations in actual scattering centers than glint 1. The target moves in the orthogonal plane to the vector around the origin. The simulation setup and results are shown below in Figs. 4 and 5.

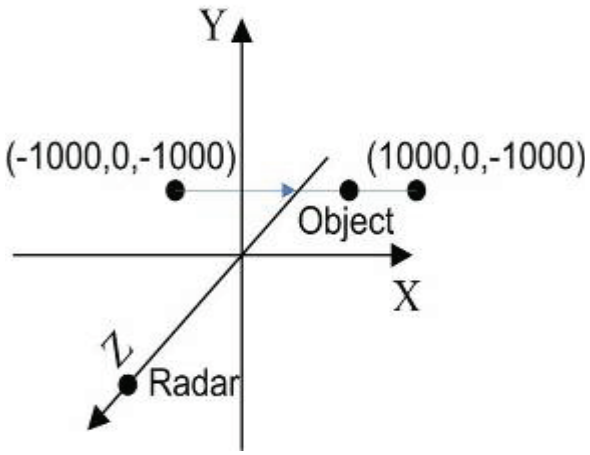

Fig. 2. Glint 1 simulation movement.

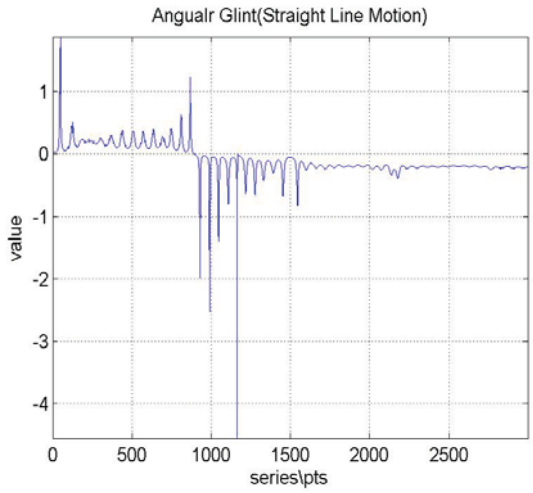

Fig. 3. Glint 1 simulation result.

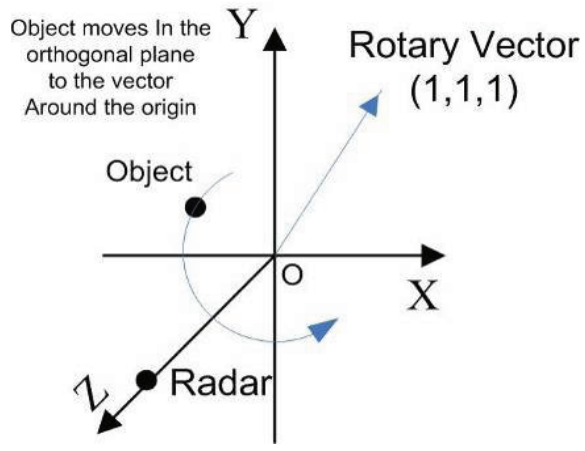

Fig. 4. Glint 2 simulation movement.

The glint simulation parameters are summarized in Table I.

Table I: Greco simulation parameters.

Motion	Straight Line	Rotary
Frequency	10 GHz	10GHz
Polarization	VV	VV
Incident Electric Field Intensity	1V/m	1V/m
Incident Direction	-Z	-Z
Calculation Plane	Azimuth	Azimuth
Glint Unit	meter	meter
Calculation Points	3600	18000

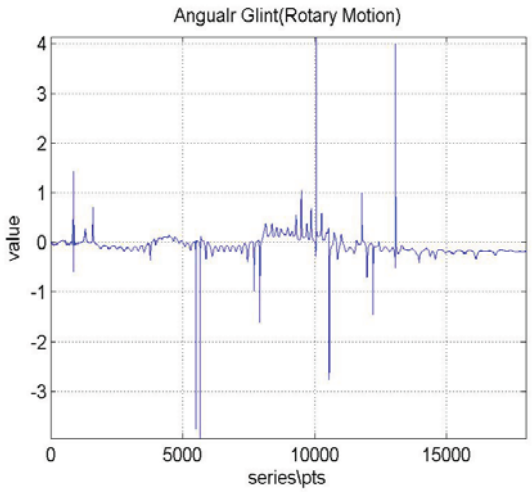

Fig. 5. Glint 2 simulation result.

III. SURROGATE DATA METHOD AND CALCULATION EXMAPLE OF LORENZ ATTRACTOR

A. Surrogate data method introduction

There are several methods to verify nonlinearity for time series. As glint calculation is done for every observation time interval in the trajectory, and can be regarded as time series. The surrogate data method can diagnose nonlinearity in noisy series and low dimension chaos, whereas typical chaotic verification approaches are unable to do so [12]. For our purpose a generalization of the typical application of this method is required. Therefore, the workflow of surrogate data method is summarized below in Fig. 6 [12].

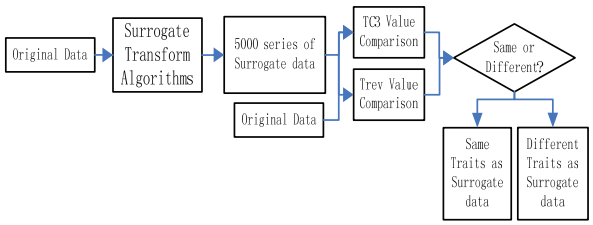

Fig. 6. Surrogate data method work flow.

The general operation of surrogate data workflow is summarized as:

1) Linear stochastic algorithms are designed (phase randomized Fourier transform and amplitude adjusted Fourier transform, PRFT and AAFT), and the original data (Lorenz or glint data) are calculated with these methods to generate a large number of surrogate data.

2) The original data and surrogated data series are measured by two statistical parameters, higher order moments and time reversibility (TC3 and Trev), whose types are specially selected for powerful nonlinear detections.

3) If the values of these parameters for original and surrogated data are notably different, the original data is nonlinear; if not, the data is linear [12]. Moreover, the powerfulness of nonlinearity is clarified by the RLCI, which is a newly proposed parameter.

B. Surrogate data generation

As angular glint is derived from nonlinear differential expressions, it is assumed that angular glint is powerfully nonlinear. For surrogate data generation, two typical algorithms to distinguish powerful nonlinear are applied: the first is PRFT (method 1) [13]. Given a time series x(t) of N values sampled by regular interval times Δt, the discrete Fourier transform can be written as,

$$X(f) = \mathcal{F}\{x(t)\} = \sum_{N=0}^{N-1} x(t_N) e^{2\pi i f n \Delta t} = A(f) e^{i\phi(f)}. \quad (9)$$

Then a random phase, which is chosen uniformly from [0, 2π] is added to the phase, and the surrogate data is given by equation (10), and this result has the same power spectrum and autocorrelation function as the original data.

$$X'(f) = F^{(-1)}(A(f) e^{i\phi(f)+i\varphi(f)}) = F^{(-1)}(X(f) e^{i\phi(f)})). \quad (10)$$

The second surrogate generation method is AAFT

(method 2) [13]. It is assumed that h is a nonlinear transform and is monotonic. Firstly h^{-1} is simulated by reordering normal white noise to the rank of x(t), then any possible nonlinear dynamics are destroyed by phase randomization (derived data set y^{FT}). Finally, h is simulated by reordering the original data to the rank order of y^{FT}.

C. The selections of test statistics

After the surrogate data have been generated, nonlinearity verification can be conducted by comparing the statistical verification parameters of the original data and the surrogate data. The two statistical parameters of TC3 and Trev are selected for powerful nonlinear diagnosis [14-16],

$$\mathrm{TC3}\left(\{x_n\},\tau\right)=\frac{\left\langle\left(x_n x_{n-\tau} x_{n-2\tau}\right)\right\rangle}{\left|\left\langle x_n x_{n-\tau}\right\rangle\right|^{\frac{3}{2}}} \tag{11}$$

$$Trev(\{x_n\},\tau)=\frac{\left\langle(x_n-x_{(n-\tau)})^3\right\rangle}{\left\langle(x_n-x_{(n-\tau)})^2\right\rangle^{(3/2)}}, \tag{12}$$

where the time lag τ is chosen by the first minimum value of the auto mutual information function of $\{x_n\}$, and $\langle x\rangle$ denotes mean values.

D. Calculation example of Lorenz attractor

The Lorenz attractor can be calculated by [14],

$$\begin{cases}\dfrac{dx}{dt}=-\sigma(y-x)\\ \dfrac{dy}{dt}=-xz+rx-y\\ \dfrac{dz}{dt}=xy-bz\end{cases}. \tag{13}$$

The time step is chosen as 0.025, and the constants σ, r, b are set as 0.1, -0.1, and 0.02, data length is 18000 and the x axis series is simulated, as shown in Fig. 7. The test statistics comparisons are shown in Fig. 8.

TC3 values are shown as appearance probability (y-axis) versus TC3 values (x-axis) in Fig. 8, and for the surrogate data (blue bars) and for original Lorenz data (red bar). Similar results are shown in Fig. 9 for AAFT surrogate method. The surrogate data method test results of Lorenz attractor are summarized in Table II. Also, the RLCIs and the overall length of all test statistical values are given. Their explanations are given in the next section.

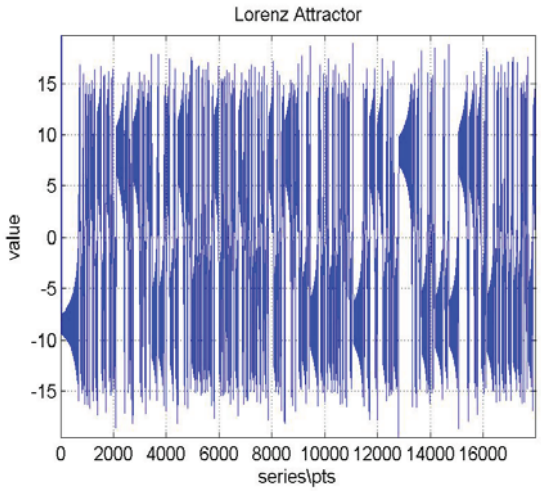

Fig. 7. Lorenz surrogate data (x series).

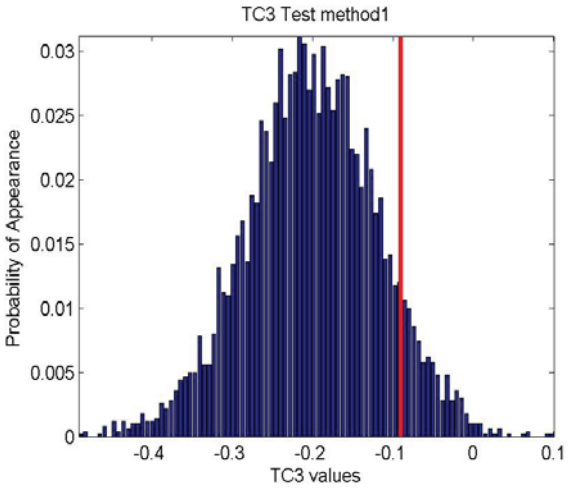

Fig. 8. Lorenz surrogate data test (PRFT, TC3).

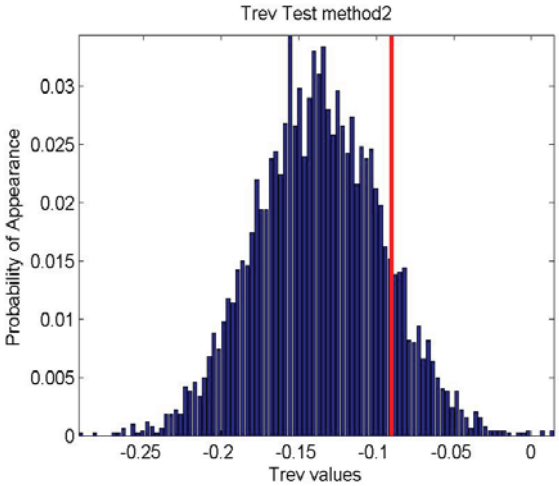

Fig. 9. Lorenz surrogate data test (AAFT, Trev).

Table II: Surrogate data results for Lorenz.

Surrogate Method	**PRFT**		**AAFT**	
Test Statistic	TC3	Trev	TC3	Trev
Test Statistic Value (Original Data)	-0.09	-0.08	-0.09	-0.08
Confidential Interval	-0.16~ -0.26	-0.16~ -0.25	-0.12~ -0.17	-0.12~ -0.17
RLCI	□□□ □□	□□□ □□	14.3%	16.7%

Table III: Surrogate tests for straight-line glint.

Surrogate Method	**PRFT**		**AAFT**	
Original Data	**Straight-Line Glint**			
Test Statistic	TC3	Trev	TC3	Trev
Value (Original Data)	-0.46	-0.44	-0.44	-0.45
Confidential Interval	-0.90~ -0.71	-0.90~ -0.78	-0.90~ -0.58	-0.98~ -0.52
RLCI	□□□ □	□□□ □	8.3%	12.4%

Table IV: Surrogate tests for rotary glint.

Surrogate Method	**PRFT**		**AAFT**	
Original Data	**Straight-Line Glint**			
Test Statistic	TC3	Trev	TC3	Trev
Value (Original Data)	-0.61	-0.60	-0.60	-0.58
Confidential Interval	-1.30~ -0.91	-1.40~ -0.90	-0.90~ -0.70	-1.00~ -0.70
RLCI	□□□ □□	□□□ □□	8.1%	10.2%

E. Nonlinear verification criterion

From canonical references and Lorenz model, the verification criteria for powerful nonlinearity are concluded as [15-17]:

1) The test statistics values of the original data are different from the values of surrogated data, or more precisely, they fall outside the confidence intervals of the values of surrogated data. The boundary of intervals can be determined by a probability range (in this case ≥ 0.025).

2) The RLCI defined in equation (13) are in inverse ratio of the intensity of nonlinearity. If the RLCI values are smaller than the results of Lorenz model (shown in Table II), it can be determined that they are more powerfully nonlinear than Lorenz,

$$\mathrm{RLCI} = \frac{\mathrm{length(confidence\ interval)}}{\mathrm{length(all\ values)}}. \qquad (14)$$

It can be seen from Table II that TC3 and Trev values of the Lorenz data all fall outside the surrogate data confidence intervals. Also, the RLCI values are shown. The results show that Lorenz data are powerfully nonlinear, and agree with common sense in nonlinear science.

IV. NONLINEAR VERIFICATION OF ANGULAR GLINT SERIES BY SURROGATE DATA METHOD

The glint data simulated in Figs. 3 and 4 are verified by the surrogate data test workflow of Fig. 6. The test statistics comparisons of the straight line motion glint are shown in Fig. 10, and similar results are shown in Fig. 11 for rotary motion glint. The two surrogate test results are also summarized in Tables III and IV.

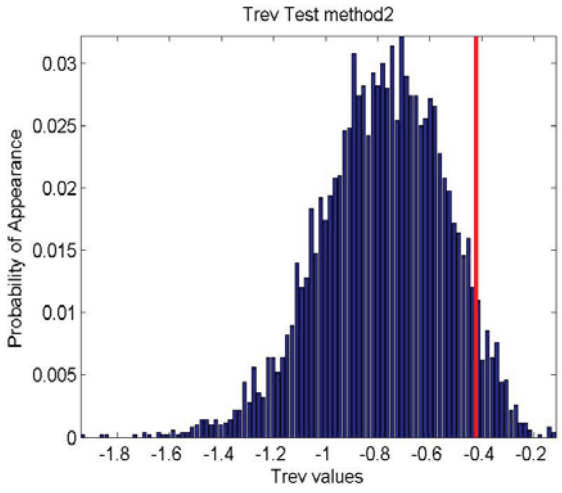

Fig. 10. Glint 1 surrogate data test (AAFT, Trev).

It can be observed that even by a narrower confidence interval boundary of probability 0.02, large differences are still clearly observed among the straight line motion glint and its surrogated data sets. In other words, the statistics values of the straight line glint fall outside the confidence intervals. Also, the RLCI values of straight line glint are smaller than Lorenz model. For rotary glint, all the TC3 and Trev values fall outside the confidence intervals of its surrogate data sets, and the RLCI values are also smaller than Lorenz.

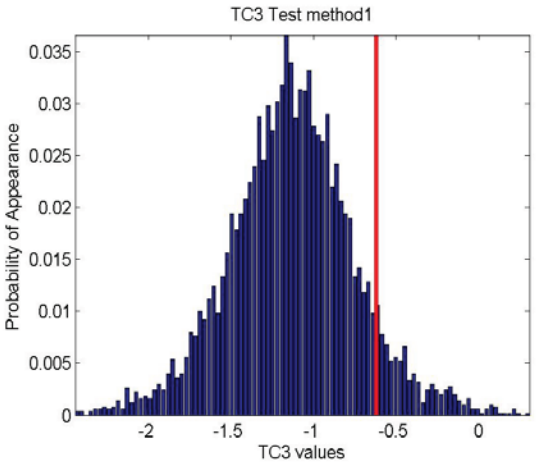

Fig. 11. Glint 2 surrogate data test (PRFT, TC3).

Therefore, considering the nonlinear verification criterion stated above, both straight line glint and rotary motion glint have been proved to possess powerful nonlinear traits, even more powerful than Lorenz model, which is a prerequisite for chaotic verifications. If angular glint is proved to be chaotic, then corresponding prediction and suppression techniques can be applied in the DSP unit of radar receivers. By these techniques, target information errors caused by angular glint can be lowered.

V. CONCLUSION

In this paper, the nonlinearity of radar angular glint is verified by the surrogate data method. Firstly, two angular glint series of a typical target are calculated by the Greco method. Secondly, the fundamentals of surrogate data method and its work flow are stated, and the nonlinearity verification criteria are demonstrated. A new verification parameter (RLCI) is proposed, and the effectiveness of this method is proved by Lorenz model. Finally, the nonlinearity traits of angular glint are proved by comparisons with the Lorenz model results and the verification criteria with all the details of nonlinear verifications are given and analyzed.

Nonlinearity is the first milestone in verifying the chaotic traits of angular glint. If nonlinearity is not proved, chaotic verification is meaningless. Even if chaos is proved without nonlinearity proof, it is not persuasive. After the nonlinear verification of angular glint, several preliminary chaotic verifications of angular glint series have been proposed with clear chaotic traits [18]. In chaotic science theories, if a time series is chaotic, then there are several ways to perform predictions and oscillation reductions. As angular glint is harmful for effective detection and could cause target loss, its predictions and reductions are critical in the radar signal processing. Therefore, the research results in this paper are nontrivial.

REFERENCES

[1] D. Howard, "Radar target glint in tracking and guidance system based on echo signal phase distortion," *Proc. of NEC*, pp. 840-849, May 1959.

[2] J. Lindsay, "Angular glint and the moving, rotating, complex radar target," *IEEE Trans. on Aerospace and Electronics Systems*, vol. 4, pp. 164-173, March 1968.

[3] J. Dunn and D. Howard, "Radar target amplitude angle and Doppler scintillation from analysis of the echo signal propagating in space," *IEEE Trans. on Microwave Theory and Techniques*, vol. 16, no. 9, pp. 715-728, Sep. 1968.

[4] R. Sinm and E. Graf, "The reduction of radar glint by diversity techniques," *IEEE Trans. on Antenna and Propagation*, vol. 19, no. 4, pp. 462-468, 1971.

[5] R. Ostrovityanov and F. Basalov, *Statistical Theory of Extended Radar Targets*, Translated from Russian (Barton. W. F, Barton. D. K), MA: Artech House, Ch. 1-Ch. 3, 1985.

[6] G. Stadhu and A. Saylor, "A real-time statistical radar target model," *IEEE Trans. on Aero . and Electro. Systems*, vol. 21, no. 4, pp. 490-507, 1985.

[7] H. Yin, S. Deng, R. Yingzheng, et al, "On the derivation of angular glint from backscattering measurements of each relative phase," *Acta Electronica Sinica*, vol. 9, pp. 36-40, 1996 (in Chinese).

[8] H. Yin and P. Huang, "Unification and comparison between two concepts of radar target angular glint," *IEEE Trans on Aer ospace and Electronics Systems*, vol. 31, no. 2, pp. 778-783, 1995.

[9] M. Juan, M. Ferrando, and L. Jofre, "GRECO: graphical electromagnetics computing for RCS

prediction in real time," *IEEE Antennas and Propagation Magazine*, vol. 35, no. 2, April 1993.
[10] Q. Dehua, *All-band Electromagnetic Scattering Computation for Complex Targets: Method Studies and Application Software*, Ph.D Dissertation, Dept. Elect. Eng., Beijing Univ. of Aerosnautics and Astronatics, Beijing, P. R. China, 2004 (in Chinese).
[11] N. Huansheng, F. Ning, and W. Baofa, "Visual computing method of radar glint for complex target," *Chinese Journal of Electronics*, vol. 15, no. 2, pp. 356-358, 2006 (in Chinese).
[12] D. Prichard, "Generating surrogate data for time series with several simultaneously measured variables," *Physical Review Letters*, vol. 73, no. 7, August 1994.
[13] D. Kugiumtzis, "Surrogate data test for nonlinearity including nonmonotonic transforms," *Physical Review E*, vol. 62, no. 1, pp. 25-28, July 2000.
[14] C. Merkwirth, U. Parlitz, et al. "TSTOOL User Manual," Version 1.11, 2002.4.[2011.10.13].
[15] T. Schreiber and A. Schmitz, "Surrogate time series," *Physica D*, vol. 142, pp. 346-382, 2000.
[16] J. Theiler, et al, "Using surrogate data to detect nonlinearity in time series in: nonlinear modeling and forecasting SFI studies in the sciences of complexity," vol. 7, Reading, MA: Addospm-Wesley, pp.163-188.
[17] D. Kugiumtzis, "Statically transformed autoregressive process and surrogate data test for nonlinearity," *Physical Review E* , vol. 66, 025201(R), 2002.
[18] J. Zhang and J. Miao, "The verification of chaotic characteristics of radar angular glint," *Progress in Electromagnetic Research B*, vol. 43, pp. 295-311, 2012.

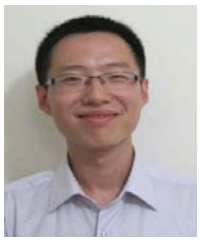

Jin Zhang was born in Beijing, P. R. China, in 1985. He received his B.S and M.S degrees from school of electronic and information engineering, Beijing University of Aeronautics and Astronautics, in 2007 and 2010. He is now pursuing for his Ph.D degree in the same institute, and majors in radar and radiometer system design.

He is interested in radar detection and target characteristic researches, and is also engaged in developing synthetic aperture interferometric radiometer imagers, which are applied in security checks. He is also doing researches in millimeter-wave FOD radar designs, in the lab of electromagnetic engineering. He has published 5 papers in the areas of radar target glint, radiometer imager design and FOD radar theories and applications.

Zhiping Li was born in 1982, in Shandong province, P. R. China. She received her B.S degree in Northwestern Polytechnic University in Shan'Xi province, and her Ph.D degree from school of electronic and information engineering, Beijing University of Aeronautics and Astronautics in 2010. She is now working as a teacher and tutor of M.S in the lab of electromagnetic engineering.

She is interested in radar system design, remote sensing and synthetic aperture interferometric radiometer and imager design and related theories and applications, especially in RCS and black body theories. She has published 8 papers in related areas.

Cheng Zheng was born in 1983, in Beijing, P. R. China. He received his B.S degree in 2006 from school of electronic and information engineering, Beijing University of Aeronautics and Astronautics, and now is pursuing his Ph.D degree in the same institute, and majors in radar and radiometer system design.

He is interested in radar system design, remote sensing and synthetic aperture interferometric radiometer and imager design and related theories and applications, especially in digital signal processing researches of these systems. He has published 4 papers in radar system, radiometer theory and digital signal processing areas.

Jungang Miao was born in 1963, in Hebei province, P. R. China. He received his B.S in 1982, in the National Defense University in Hunan province, and received his Ph.D in Bremen University, Germany, in 1998. He worked as a Professor in the remote sensing research institute of Bremen University until 2003, when he came to school of electronic and information engineering, Beijing University of Aeronautics and Astronautics. He works as a Professor and head of electromagnetic engineering lab up to the present.

He is interested in microwave and millimeter-wave radiation, diffraction and near-field detection, remote sensing, radar system, signal processing, antenna and electromagnetic calculations, and has published more than 50 papers in international journals and conferences.